EDDY CURRENT NDT AND DEEP FLAWS.

F. THOLLON
CEGELY - UPRESA 5005
Ecole Centrale de Lyon
69131 Ecully Cédex- France.
E-mail: thollon@trotek.ec-lyon.fr.

Abstrac¾ **Eddy current NDT and NDE are ever more used for applications that need important sensitivity and resolution. The design of eddy current devices by must be realized by using modelization. The large number of electromagnetic and geometrical parameters of these systems implies many simulations, and the quantity of obtained results does not allow to conceive rapidly the most effective system. To achieve such a design, we need in particular two tools, a 3D model of flaws and an automatic optimization algorithm. We propose an experimental equipment for validating a fast 3D flaw model.**

I. INTRODUCTION

Fig. 1 shows an example of structure to control in aeronautical industry. This is a screwed or riveted assembly. The materials are aluminum alloy for the sheets and titanium for the screws. Flaws can appear at great depth (below the first sheet) and along a known direction. In this case, ultrasonics cannot be used, because of a seal between the two sheets. We have to use in this case eddy currents method to control the assembly. Because of the great depth of the flaw, the obtained signal is very low-level. The aim of this problem is to be able to optimize the dimensions of the coil and the excitation current to have the highest level of the signal as possible.

A probe has been designed in our laboratory. It has been demonstrated that pulsed eddy currents [1] must be used and that the measured quantity must be the flux density at the surface of the assembly. These results have been obtained with the following methodology.

First, a 3D study has been necessary to understand eddy currents distribution near the flaw and the influence of this perturbation on sensor response [2]. It has allowed to conclude, in particular, that flux induction measurement is more effective than impedance measurement. Unfortunately, solving time are very great, and only sinusoidal current can be modelized.

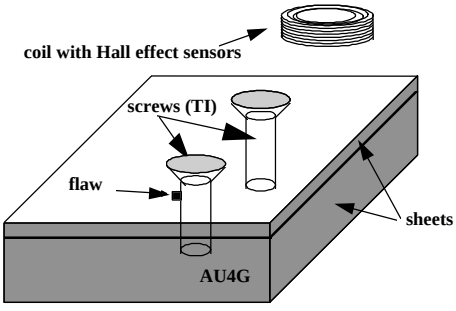

Fig. 1: eddy current NDT of screwed assemblies.

In a second step, an automatic design has been executed [3]. Because of the two previous remarks, a genetic algorithm has been implemented in a 2D FEM electromagnetic package. The obtained results show that this method is good adapted. Indeed, geometrical parameters of the sensors and current shape are automatically obtained. Moreover, one of the main advantage of this method is its easy implementation.

This methodology has been validated experimentally. The designed sensor is more effective than those already existing.

But, it has two main inconvenients:

- The use of 3D only for the knowledge of the physical phenomena for a sinusoidal current.
- The use of automatic design only with a 2D model.

To improve the efficiency of the sensor in particular:

- to be able to characterize the flaw (depth and sizes),
- to increase the detection depth,

a 3D automatic optimization must be envisage. Therefore, we must have:

- An fast model of a 3D flaw with pulsed or sinusoidal current.
- An automatic optimization method.

The main objective is to have a tool fast enough to design efficiently an eddy current probe. We propose a test equipment for validating the flaw model with the aim of characterizing it.

II.3D FLAW MODEL.

The eddy currents are created by a cylindrical coil. The screw and the coil are coaxial. During the control, the coil doesn't move.

The measurement is made with two Hall effect sensors (HES) located symmetrically in relation to the axis of the screw. These HES measure the horizontal radial component of the flux density. One HES is above a region without a flaw, the other, above a region supposed with a flaw (the flaw and the HES are in the same plane). The measured quantity is the difference between the tensions provided by the two HES. This quantity represents the horizontal differential flux density (HDFD).

A.Test equipment description.

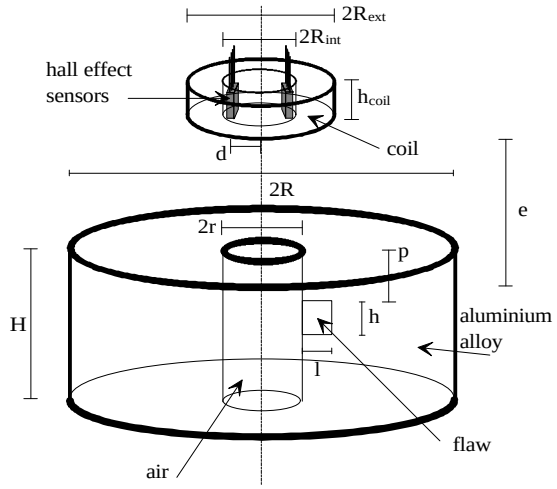

Fig. 2: Coil with HES and aluminum cylinder with a flaw.

The studied structure is simplified as shown Fig. 2: an eddy current probe above an aluminum cylinder with an artificial flaw. The screw is replaced with air. The cylinder sizes are given table 1.

1) Eddy current probe.

This is "a pancake coil" [2]. The coil sizes and the position of the HES are given table 2. The maximum value for a sinusoidal current is 500mA RMS, and for a pulsed current, 5A peak. The sensor has been calibrated:

$$\text{signal (V)} = 27.74((23.61B_1 - 0.0012) - (23.606B_2 - 0.001))$$

where signal is the measured quantity, B_1 the horizontal radial flux density measured by one HES and B_2 the horizontal radial flux density measured by the other one.

2) Standard flaws.

In order to characterize the flaw, three standard flaws, at the same depth, with the same volume but with different dimensions are used. The lengths, heights and depths are given table 3. The width of each flaw is 0.3mm.

TABLE 1

CYLINDER DIMENSIONS.

2R	2r	H	aluminum alloy conductivity
50.00 mm	10.00 mm	20.00 mm	22.7MS/m

TABLE 2

COIL DIMENSIONS AND POSITION OF HES.

$2R_{ext}$	$2R_{int}$	h_{coil}	d	e	turns number	wire diameter
24.7mm	13.0 mm	3.95 mm	5 mm	0.5 mm	445	0.2 mm

TABLE 3

AVAILABLE STANDARD FLAWS

	p (mm)	h(mm)	l(mm)	w(mm)
flaw 1	2	1	4	0.3
flaw 2	2	2	2	0.3
flaw 3	2	4	1	0.3

3) Coil supply.

The coil can be supplied either with a sinusoidal current, either with a pulsed current. We have a current generator with a 10kHz bandwidth and a maximal value of 7A. It is controlled with a tension that has the same shape than the desired current.

B. Item to compare.

We wish to compare HDFD for a current described Fig. 3. In this case, only the current turn-off is interesting (separation between excitation and material response).

Fig. 4, Fig. 5 and Fig. 6 give the experimental responses obtained with the three flaws. They represent HDFD once the current has been turned off. Numerical values are given table 4. Only high frequencies have been rejected. No other numerical treatments are performed.

C.Discussion.

The following elements are obvious points of discussion:

- Formulations used in the different regions.
- Interface conditions.
- Computational time.
- Geometrical description of the flaw (thickness).
- For impulse excitation, solving method.

III.REFERENCES.

[1] F.THOLLON, N.BURAIS: "Modeling and characterization of Pulsed eddy currents. Application to detection of flaws in riveted assemblies in aircraft structures," *Electric and Magnetic Fields From Numerical Models to Industrials Applications*, Ed. Nicolet and Belmans, Plenum Press, pp. 261-264, 1995.

[2] J.L. RASOLONJANAHARY, F. THOLLON, N. BURAIS, X. BRUNOTTE, "Study of Eddy Currents NDT Systems in Riveted Assemblies," *IEEE Transactions on Magnetics*, Vol. 32 n° 3, may 1996, pp. 1585 - 1588 .

[3] F. THOLLON, N. BURAIS: "Geometrical optimization of sensors for eddy current NDT and NDE ," *IEEE Transactions on Magnetics*, Vol. 31 n°3, may 1995, pp. 2026-2031.

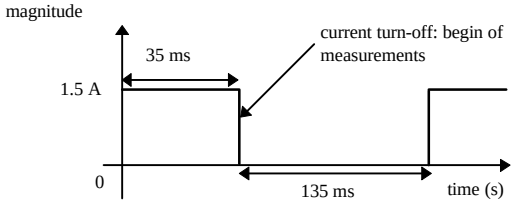

Fig. 3: Excitation signal characteristics.

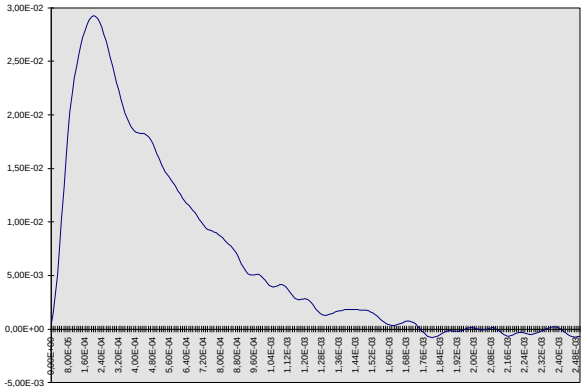

Fig. 4: Response to a current turn-off.
Flaw 3 characteristics (length*heigth): 1*4mm.

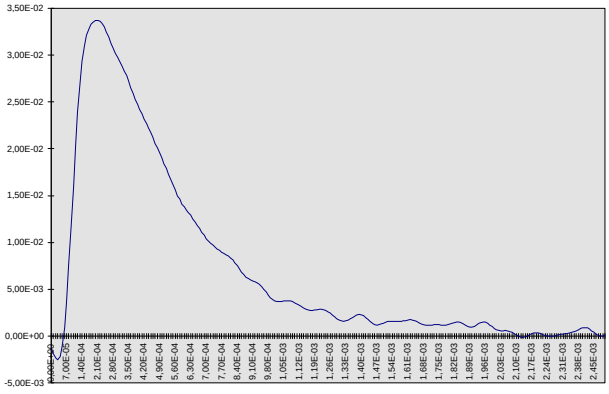

Fig. 5: Response to a current turn-off.
Flaw 2 characteristics (length*heigth): 2*2mm.

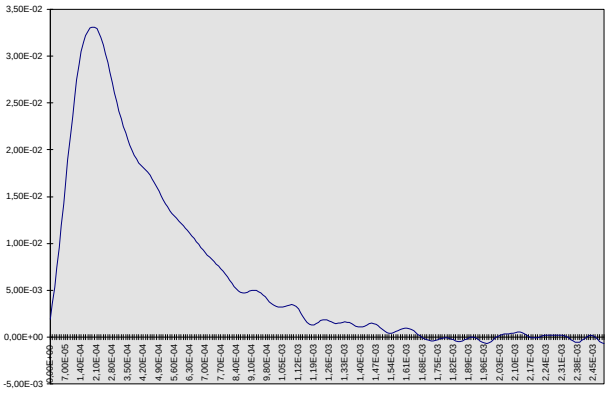

Fig. 6: Response to a current turn-off.
Flaw 3 characteristics (length*heigth): 4*1mm.

TABLE 4
HDFD (IN T) FOR THE THREE FLAWS VERSUS TIME

time (s)	HDFD for flaw 3 (T)	HDFD for flaw 2 (T)	HDFD for flaw 1 (T)
0.00E+00	6.6294E-07	-2.0469E-06	2.9786E-06
5.00E-05	1.5733E-05	-1.7261E-06	1.8177E-05
1.00E-04	3.3605E-05	2.444E-05	3.5896E-05
1.50E-04	4.1548E-05	4.7353E-05	4.8116E-05
2.00E-04	4.4756E-05	5.1477E-05	5.056E-05
2.50E-04	4.2159E-05	4.9644E-05	4.6283E-05
3.00E-04	3.6355E-05	4.5367E-05	3.834E-05
3.50E-04	3.0856E-05	4.1548E-05	3.223E-05
4.00E-04	2.8106E-05	3.6966E-05	2.8412E-05
4.50E-04	2.7801E-05	3.3147E-05	2.6426E-05
5.00E-04	2.5051E-05	2.9023E-05	2.3065E-05
5.50E-04	2.1996E-05	2.4746E-05	2.0163E-05
6.00E-04	1.9705E-05	2.108E-05	1.8177E-05
6.50E-04	1.7566E-05	1.8636E-05	1.6039E-05
7.00E-04	1.5581E-05	1.5886E-05	1.3778E-05
7.50E-04	1.4114E-05	1.4206E-05	1.193E-05
8.00E-04	1.3259E-05	1.3014E-05	9.7913E-06
8.50E-04	1.1823E-05	1.0937E-05	7.4848E-06
9.00E-04	9.3025E-06	9.1497E-06	7.4695E-06
9.50E-04	7.7139E-06	8.0805E-06	7.2098E-06
1.00E-03	7.3931E-06	5.9573E-06	5.4685E-06
1.05E-03	6.0031E-06	5.7281E-06	4.888E-06
1.10E-03	6.2933E-06	5.4532E-06	5.1782E-06
1.15E-03	4.4603E-06	4.4145E-06	2.8564E-06
1.20E-03	4.3228E-06	4.2923E-06	2.1843E-06
1.25E-03	2.8564E-06	4.0173E-06	2.7801E-06
1.30E-03	1.9705E-06	2.6426E-06	2.2454E-06
1.35E-03	2.4898E-06	2.8106E-06	2.3524E-06
1.40E-03	2.7953E-06	3.4674E-06	1.6192E-06
1.45E-03	2.7648E-06	2.1232E-06	2.2454E-06
1.50E-03	2.5815E-06	2.0927E-06	1.2419E-06
1.55E-03	1.5733E-06	2.3982E-06	7.6833E-07
1.60E-03	5.8045E-07	2.5509E-06	1.4496E-06
1.65E-03	7.7444E-07	2.3829E-06	7.5E-07
1.70E-03	1.0906E-06	1.7261E-06	-4.8727E-07
1.75E-03	-2.1996E-07	1.833E-06	-3.9257E-07
1.80E-03	-1.2037E-06	1.9858E-06	-2.108E-07
1.85E-03	-5.667E-07	2.1385E-06	-6.996E-07
1.90E-03	-2.6731E-07	1.4786E-06	-4.1701E-08
1.95E-03	-9.0886E-08	2.3065E-06	-8.2332E-07
2.00E-03	1.361E-07	1.2403E-06	-4.2006E-07
2.05E-03	-7.2404E-08	9.0428E-07	4.7658E-07
2.10E-03	8.0041E-08	1.3427E-07	7.6375E-07
2.15E-03	-9.6385E-07	4.1854E-08	3.2841E-07
2.20E-03	-5.8351E-07	4.888E-07	-9.4705E-08
2.25E-03	-6.7668E-07	-2.9175E-08	3.223E-07
2.30E-03	-5.1477E-07	2.9481E-07	2.8106E-07
2.35E-03	1.6192E-07	5.8656E-07	-3.9868E-07
2.40E-03	1.5733E-07	1.3411E-06	-5.6823E-07
2.45E-03	-9.44E-07	6.0336E-07	1.7414E-07
2.50E-03	-1.0723E-06	1.6497E-07	-1.0861E-06